

Original Article

Portal vein tumor thrombus is more sensitive to irradiation

Long Zhang^{1*}, Nan Li^{2*}, Shuang Feng^{2*}, Hao Wang², Yu-Fu Tang³, Hong-Ming Yu², Wei-Xing Guo², Jie Shi², Yan Meng², Shu-Qun Cheng²

¹Xinxiang Central Hospital, Henan 453000, China; ²Eastern Hepatobiliary Surgery Hospital, Second Military Medical University, Shanghai, China; ³Department of Hepatobiliary Surgery, General Hospital of Shenyang Military Area Command, Liaoning, China. *Equal contributors.

Received June 21, 2016; Accepted November 30, 2016; Epub March 15, 2017; Published March 30, 2017

Abstract: Purpose: To study the changes of biological behavior in PVTT cells after irradiation. Methods: PVTT-originated cells CSQT-2 were compared with the HL-7702 human liver cell line, Hep3B and Huh7 human HCC cell lines on irradiation biology parameters and irradiation-related biological behavior, including apoptosis, proliferation and metastasis and other related mechanisms *in vitro*. We further assessed the radiosensitivity of xenograft *in vivo*. Results: Irradiation biology parameters of CSQT-2 cell were less than that of HCC cells; irradiated CSQT-2 cells had a higher prevalence of apoptosis and death, a higher rate of proliferation inhibition, and a weakened migration capacity compared with HCC cell lines. In addition, CSQT-2 cells had a higher rate of activated apoptotic proteins which arrested cell cycles in the G2/M phase, including PARP and caspase3, and a decreased rate of PCNA expression. Importantly, irradiation induced more severe shrinkage in the xenograft tumor derived from CSQT-2 cells compared with derived from Huh7 cells. Conclusions: Our results demonstrated that PVTT-originated cells were more radio-sensitive than HCC cells both *in vitro* and *in vivo*, which supported the application of radiotherapy for HCC patients with PVTT in clinical settings.

Keywords: Portal vein tumor thrombus, hepatocellular carcinoma, irradiation

Introduction

Hepatocellular carcinoma (HCC) is the fifth most common malignancy and the third leading cause of cancer-related death worldwide [1, 2]. Portal vein tumor thrombus (PVTT) is a major complication of HCC and is associated with poor prognosis [3]. Previous studies have reported that the median survival of patients with portal venous invasion was 2.7-4 months if they received no treatment [4, 5]. Moreover, approximately 40.5-90% of advanced HCC has been found to accompany by PVTT [6, 7]. Thus, developing effective therapeutic strategies for PVTT is crucial for improvement of HCC prognosis.

In the past decade, several treatments including surgical resection, transarterial chemoembolization (TACE), radiotherapy (RT), percutaneous local ablative therapy and molecular target-drugs have been used to cure HCC with PVTT.

However, due to limitations from many factors, these treatments are not applicable to all HCC with PVTT patients, and the therapeutic outcome remains discouraging [8, 9]. In recent years, irradiation therapy has become an alternative treatment, and its role has been gradually expanded from a palliative intent to a curative intent [10]. According to the related research on radiotherapy of HCC with PVTT [11-13], the objective response rate was 35.6%-75%, and the median survival was 7.5-16.5 months. For example, Zeng *et al.* [11] reported on 44 patients who received external beam irradiation therapy, 15 (34.1%) showed complete disappearance of tumor thrombi, 5 (11.4%) were in partial remission, and the median survival was 8 months versus 4 months for the non-EBRT group.

Despite its clinical importance, the modulation of the biological behavior of PVTT cells induced by RT is still largely obscure. In this study, we

Radiosensitivity of PVTT

compared the different biological behaviors among normal liver cells, HCC cells and PVTT-originated cells, treated or untreated with RT.

Materials and methods

Samples

Human tumor tissues and computed tomography (CT) scan images of 6 HCCs with PVTT were obtained from the Eastern Hepatobiliary Surgery Hospital during 2012-2013 after obtaining informed consent. All 6 patients underwent a hepatectomy after 3D-CRT. The presence of PVTT was histopathologically confirmed in the resected specimens.

Cell lines and reagents

The human liver cell line HL-7702 and the human HCC cell lines, Hep3B and Huh7, were obtained from the Cell Bank of the Shanghai Institutes for Biological Sciences (Chinese Academy of Sciences, Shanghai, China). The PVTT-originated cell line CSQT-2 was established and preserved by our laboratory [14]. They were grown in DMEM (Gibco Invitrogen, Grand Island, NY, USA) supplemented with 10% fetal bovine serum (Gibco Invitrogen) and maintained in a humidified 37°C incubator with 5% CO₂. Antibodies for immunoblotting such as cleaved caspase-3 and procaspase-3 were purchased from Cell Signal Technology (Beverly, MA, USA). Other antibodies such as Bcl-2, cleaved PARP, PCNA, and β-actin were purchased from EPITOMICS (Burlingame, CA, USA).

Colony formation assay

Variable numbers of cells from 300 to 10,000 were plated into 6-well plates. After 24 h culture, the cell dishes were sealed with sealing membrane and the cells irradiated with 0, 2, 4, 6, 8 and 10 Gy X-ray radiation (6 MV, the dose rate was 400 cGy/min) by a Linear Accelerator System (ELEKTA, Shanghai, China) at room temperature. After irradiation, the cells were incubated for 7 days. Colonies were fixed with 37% formaldehyde solution and stained with crystal violet, and colonies of more than 50 cells were counted. Furthermore, the survival fraction was determined by measuring the colonies after irradiation exposure and dividing by the plating efficiency. The average data were fitted into a single hit multi-target formula: $SF=1-$

$(1-e^{-D/D_0})^N$. IBM SPSS 20 software was used to fit the cell survival curve as well as the irradiation biological parameters, including the average lethal dose (D_0), the quasi-threshold dose (D_q), and extrapolation number (N).

Flow cytometric analysis of apoptosis and cell cycle

Apoptotic and dead cells were quantified using an Annexin V-FITC/PI detection kit according to the manufacturer's instructions (eBioscience, San Diego, CA, USA). Analyses were performed by a flow cytometer (MACS). FITC-positive and PI-negative cells were regarded as apoptotic cells, FITC-negative and PI-positive cells were regarded as dead cells. Cell cycle distribution detection: cells were harvested and fixed overnight with 70% ethanol at 4°C. After fixation, the cells were incubated with 250 μL PI (20 μg/ml) solution containing RNase A (1 mg/ml) in the dark. Cellular DNA content was determined on a flow cytometer.

Cell viability/toxicity assay

After irradiation, cells were reseeded and cultured on a 96-well plate. Cell viability/toxicity was measured using Cell Counting Kit-8 (Dojindo Molecular Technologies, Gaithersburg, MD) according to the manufacturer's instructions. The optical density (OD) at a wavelength of 450 nm was measured by a microplate reader. Each experiment containing three replicates was repeated three times.

Western blotting

Cells were rinsed with PBS and lysed in RIPA buffer (Thermo, Waltham, MA, USA) containing 1 mmol/L phenylmethylsulfonyl fluoride for 30 min on ice. Protein concentration was determined by BCA protein assay kit (Thermo). Equal amounts of protein were loaded on 10% SDS-PAGE gels, transferred onto polyvinylidene difluoride membranes (Millipore, Bedford, MA), and blocked with 5% skim milk for 1 h at room temperature. The membrane was incubated with primary antibody overnight at 4°C. After washing, the membrane was incubated with the appropriate secondary antibody (Promega, Madison, WI, USA) for 1.5 h. The blots were visualized by using ECL Western blot detection reagent (Thermo) and scanned by a chemiluminescence imaging analyzer (image Quant LAS 4000, GE Company, Fairfield, CT, USA).

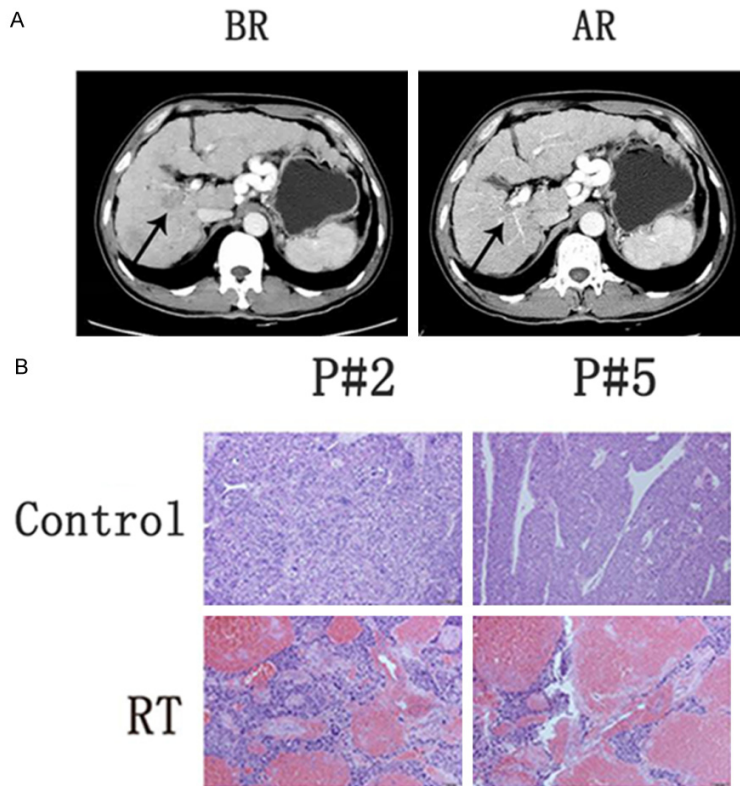


Figure 1. Representative images of clinical CT scans before and after radiotherapy for HCC with PVTT patients and HE staining of the indicated groups. A: Representative clinical CT scan images before and after radiotherapy in HCC with PVTT patients. BR: CT scan images before radiotherapy; AR: CT scan images one month after radiotherapy. B: Representative photomicrograph of HE staining of the indicated groups. Magnification 100 \times . Control: non-radiotherapy group (directly to surgical resection); RT: radiotherapy group (surgical resection after radiotherapy); P#, specimen number.

Establishment of the tumor xenograft model and irradiation

Five-week-old male BALB/c nude mice were purchased from Animal Research Center, Second Military Medical University (Shanghai, China). Mice were maintained under standard conditions and treated according to the institutional guidelines for animal care. The establishment of the PVTT xenograft model was performed as described by Feng YX [15]. We obtained fresh PVTT specimens from clinical hepatectomies and orthotopically implanted them into the livers of the nude mice. Then, we succeeded in establishing the xenograft models, which were used as successive transplantable tumor lines. One of the xenograft lines, named PVTT-#A, was able to grow in cultures, and the cells were used to establish a subcutaneous xenograft tumor model. PVTT-#A and Huh7 cells were resuspended in 100 μ l of FBS-

free culture medium and subcutaneously injected into the backs of mice at 2×10^6 cells/mouse. Tumor size was measured using calipers, and tumor volume was calculated as $(\text{length} \times \text{width}^2) / 2$. The animals were immobilized in custom-designed jigs with only the right back exposed to an X-ray beam. A total dose of 18 Gy was delivered in 6 fractions performed 2 weeks after injection of cells, and tumor size was measured every 3 days thereafter. The shrinkage ratio of the xenograft tumors was calculated as $(\%) = [V(\text{BR}) - V(\text{RT})] / V(\text{BR})$, in which V(BR, RT) indicates the tumor volume of the before radiotherapy group (BR) and irradiation group (RT), respectively. Each group had 6 mice.

H&E staining and immunohistochemical staining for tissue specimens

The fresh human tumor tissues from HCC with PVTT patients treated with surgery resection after 3D-CRT and surgery resection directly were fixed with formalin and

embedded with paraffin. Then, the tissues were cut into slices and mounted on slides for H&E staining and immunohistochemical staining. Following deparaffinization, the sections were permeabilized with a 0.1% Triton X-100 solution in PBS for 30 min. Sections were then blocked for 1 h at room temperature with 2% goat serum and 1% BSA in PBS and incubated with primary antibody overnight at 4 $^{\circ}$ C. Sections were then rinsed in PBS and incubated with appropriate secondary for 1 h at room temperature. Negative control slides omitting the primary antibodies were included in all assays. The signals were developed with avidin-biotin-peroxidase complexes with a DAB substrate solution. Images were taken by microscope.

Wound healing assay and transwell migration assay

Cells were seeded onto 6-well plates and cultured to confluence. Scratch wounds were cre-

Radiosensitivity of PVTT

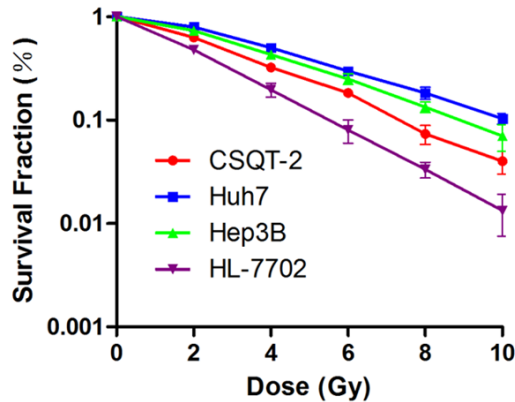


Figure 2. Dose survival curves of HL-7702, Hep3B, Huh7 and CSQT-2 cells. The average survival fraction data were obtained from a clone formation assay fitted into the following single-hit multi-target formula: $S=1-(1-e^{-D/D_0})^N$, and SPSS 20 software was used to fit the cell survival curves. Points, the mean survival fraction from three replicates; Bars, SD.

Table 1. The irradiation biological parameters of the cells

Cell	Irradiation biology parameters		
	D_0	N	D_q
HL-7702	2.16±0.14	1.29±0.14	0.53±0.25
Hep3B	3.15±0.15*	1.75±0.12*	1.74±0.20*
Huh7	3.42±0.16**	1.91±0.24**	2.19±0.31**
CSQT-2	2.81±0.09	1.45±0.07	1.05±0.16

D_0 : the average lethal dose, D_q : the quasi-threshold dose, N: extrapolation number. * $P<0.05$, ** $P<0.01$ versus CSQT-2. Data are presented as the mean ± SD of three independent experiments.

ated with a 10 µl pipette tip. The wounds were photographed with a phase-contrast microscope at 0 h and 24 h. Cell migration was quantitated by measuring the width of the wounds. Migration was calculated as (%)=[W(OW)-W(con or RT)]/W(OW), in which W(OW, con, RT) indicates the original wound width, the wound width of non-radiation group, the wound width of radiation (6 Gy) group after 24 h or 72 h, respectively. A total of 5 areas were randomly selected in each well. The experiments were performed with at least 3 replicates. Boyden chambers (8 µm pore size polycarbonate membrane) were obtained from Corning Corporation (Toledo, OH, USA). Cells (1×10^5) in 0.2 mL of serum-free medium were placed in the upper chamber, and the lower chamber was loaded with 0.8 mL of medium containing 10% fetal

bovine serum. After 24 h of incubation at 37°C with 5% CO₂, cells that migrated through the filter membrane of the Boyden chamber were fixed with paraformaldehyde, stained with 4'-6-diamidino-2-phenylindole (DAPI), and photographed by fluorescence microscope; five fields of each well were counted. The experiments were repeated thrice.

Statistical analysis

All data are presented as the mean ± SD. Student's t test was used for the comparison of measurable variants of two groups in IBM SPSS 20 statistics software unless otherwise indicated (Mann-Whitney U test). $P<0.05$ was defined as statistically significant.

Results

Radiotherapy strongly reduces the size of PVTT in HCC patients

To investigate the effect of radiotherapy on patients with PVTT, we collected CT scan images of six HCC patients with PVTT treated with irradiation. The CT scan images before and after irradiation showed that the size of PVTT declined more than the primary tumor (**Figure 1A**). We also employed the pathological HE dyeing test in 6 cases of fresh specimens of PVTT. We still found that a focal area of necrosis emerged in these cases (**Figure 1B**). These results confirmed the exact efficacy of radiotherapy on PVTT.

CSQT-2 cells are more sensitive to irradiation

Irradiation biology parameters are an important index of radiosensitivity. We examined survival curves (**Figure 2**) and irradiation biology parameters (**Table 1**) in PVTT-originated cells (CSQT-2), HCC cells (Hep3B and Huh7) and normal hepatocytes (HL-7702) through colony formation assay. The survival fraction of CSQT-2 in multiple doses was lower than that of Hep3B or Huh7 ($P<0.05$). Irradiation biology parameters of CSQT-2, including extrapolation number (N), which represents the width of the dose survival curve shoulder, mean lethal dose (D_0), and quasi-threshold dose (D_q), were less than those of Hep3B and Huh7 ($P<0.05$). The results suggested that CSQT-2 cells have superior sensitivity relative to Hep3B and Huh7.

Radiosensitivity of PVTT

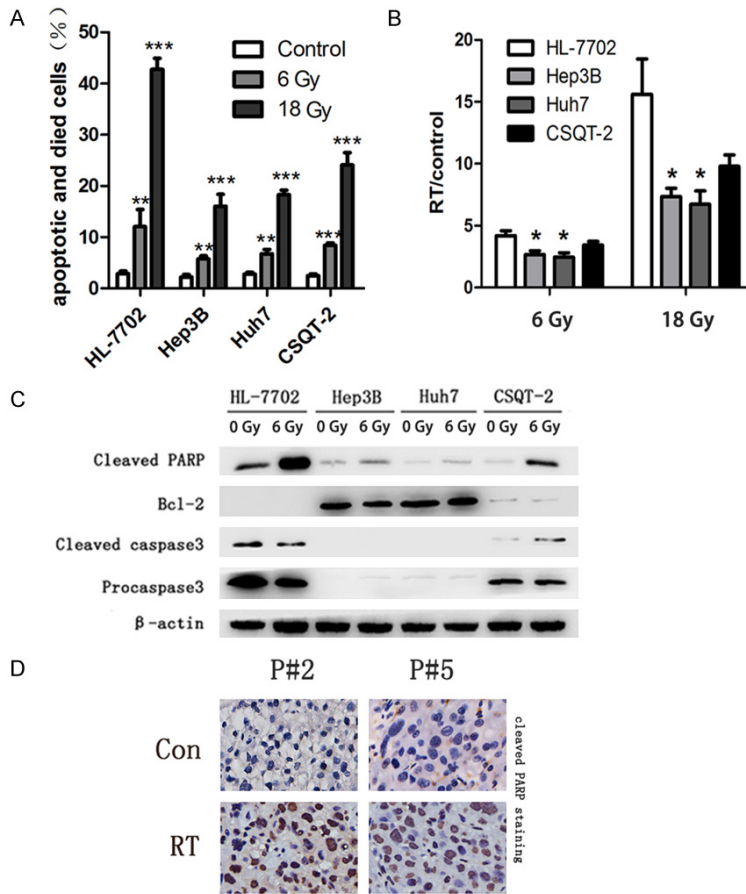


Figure 3. Irradiation causes a high proportion of apoptosis and death in CSQT-2 cells. A: The apoptotic and dead cells were detected by flow cytometry 72 h after irradiation with a single dose of 6 Gy and total dose of 18 Gy. The results were expressed as the mean \pm SD of three independent experiments. ** $P < 0.01$, *** $P < 0.001$ versus the control group. B: The respective bar graphs show the ratio of apoptosis and dead cells between the irradiation group and the control group. * $P < 0.05$ versus CSQT-2. C: Western blot analysis of caspase3, cleaved PARP, and Bcl-2 protein expression in all types of cells before and after irradiation. β -Actin was used as a loading control. D: Representative photomicrographs of the immunohistochemical assay measuring cleaved PARP in the non-radiotherapy group (control) and the radiotherapy group (RT).

Higher percentage of apoptosis is observed in CSQT-2 cells treated with irradiation

To clear whether apoptosis and death of CSQT-2 cells after irradiation could reflect their relative sensitivity, cells were treated with two types of irradiation, a single 6 Gy dose of irradiation and a fractionated irradiation with a total dose of 18 Gy in 6 fractions. As **Figure 3A** shows, the irradiation caused a certain ratio of apoptosis and death in all cell lines. The apoptosis and death rate in CSQT-2 cells after irradiation at 6 Gy and 18 Gy were $8.39\% \pm 0.50$

and $24.08\% \pm 2.40$ respectively, significantly higher than $2.48\% \pm 0.36$ of the control group (0 Gy) ($P < 0.01$). We calculated the ratio of apoptosis and death before and after irradiation to compare the difference in the degree of apoptosis and death among the four cell lines (**Figure 3B**), and the results showed that the ratio was higher in CSQT-2 cells than in Hep3B and Huh7 cells ($P < 0.05$). Exploring the mechanism of apoptosis of CSQT-2 cells after irradiation, we found that cleaved caspase3 and cleaved PARP protein levels up-regulated after irradiation through Western blot assay (**Figure 3C**), which suggested that caspase3 participates in the process of cell apoptosis after irradiation by cracking PARP. Meanwhile, we found that the level of the anti-apoptosis protein Bcl-2 was lower in CSQT-2 cells than in Hep3B and Huh7 cells, which indicates that the anti-apoptotic ability of CSQT-2 itself is weaker than that of Hep3B and Huh7 cells. In addition, we found that cleaved PARP expression in PVTT specimens is higher after radiotherapy than in the non-radiotherapy group by an immunohistochemical assay ($P < 0.001$) (**Figure 3D**).

Irradiation suppresses PVTT cell proliferation to a larger degree by arresting the cell cycle in G2/M phase and down-regulating PCNA expression

To identify whether proliferation was inhibited by irradiation and to reflect the relative sensitivity of CSQT-2 cells, we further investigated the proliferation capacity of cells after irradiation. **Figure 4A** shows the OD value of all cells that underwent 6 Gy of irradiation, and no significant difference was found between the control group in HCC cells and CSQT-2 cells.

Radiosensitivity of PVTT

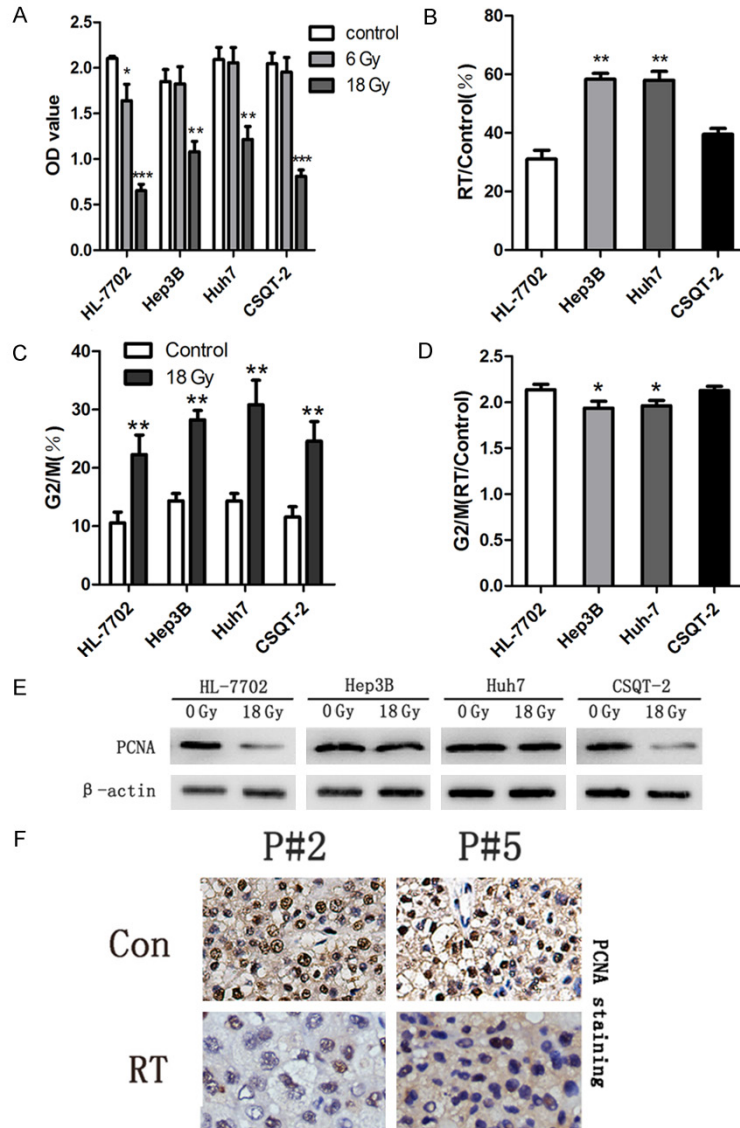


Figure 4. Irradiation inhibits proliferation of CSQT-2 cells. A: After the cells were irradiated with 6 Gy and 18 Gy, 96-well plates were incubated at 5000 cells per well and CCK-8 solution was added to each well after 72 h. OD values were measured by a microplate reader at a wavelength of 450 nm. Each bar chart represents the OD value of various cells. Each bar represents the mean with SD of three separate assays. * $P < 0.05$, ** $P < 0.01$, *** $P < 0.001$ irradiation group versus the control group. B: The OD value ratio between the irradiation group and control group. ** $P < 0.01$ versus CSQT-2. C: The ratio of the G2/M phase in four types of cells through flow cytometer detection. * $P < 0.05$, ** $P < 0.01$ RT group versus the control group. D: Histogram showing the ratio of G2/M phase between the irradiation group (18 Gy) and the control group. * $P < 0.05$. E: Western blotting analysis of PCNA protein expression in cells that did or did not undergo irradiation with 18 Gy. β -Actin was used as a loading control. F: Representative photomicrographs of the immunohistochemical assay measuring PCNA in the control group and RT group. P#, specimen number.

ty, we calculated the ratio of the OD value between the irradiation group (18 Gy) and the control group (Figure 4B). The rate of the CSQT-2 cells was 39.50 ± 1.99 , less than 58.30 ± 2.01 in Hep3B and 57.96 ± 3.03 in Huh7 cells ($P < 0.01$), which showed that the toxicity of irradiation was stronger on CSQT-2 cells than on Hep3B and Huh7 cells. In addition, we explored how irradiation inhibited proliferation. Flow cytometer detection (Figure 4C) showed that the ratio of G2/M phase was higher in CSQT-2 cells after irradiation than in the control group ($P < 0.01$). This finding showed that arresting the cells in the G2/M phase by irradiation reduced proliferation inhibition. To compare the difference, we calculated the ratio of cells in the G2/M phase between the irradiation group (18 Gy) and the control group (Figure 4D). The ratio in CSQT-2 cells was 2.13 ± 0.05 , higher than 1.94 ± 0.07 in Hep3B and 1.96 ± 0.06 in Huh7 cells ($P < 0.05$). Moreover, we found that PCNA expression in CSQT-2 cells was down-regulated by measuring PCNA expression using a Western blot (Figure 4E). Meanwhile, PCNA expression in the PVTT specimens was lower after radiotherapy than in the non-radiotherapy group by immunohistochemical assay (Figure 4F). This finding indicated that PCNA participates in irradiation-induced inhibition of proliferation.

PVTT is more sensitive to irradiation in nude mice than the HCC primary tumor

However, the OD values of all cells that underwent 18 Gy of irradiation were less than that of control group ($P < 0.001$). To compare the toxic-

To further validate the sensitivity of PVTT to radiotherapy *in vivo*, we established a subcutaneous xenograft tumor model derived from

Radiosensitivity of PVTT

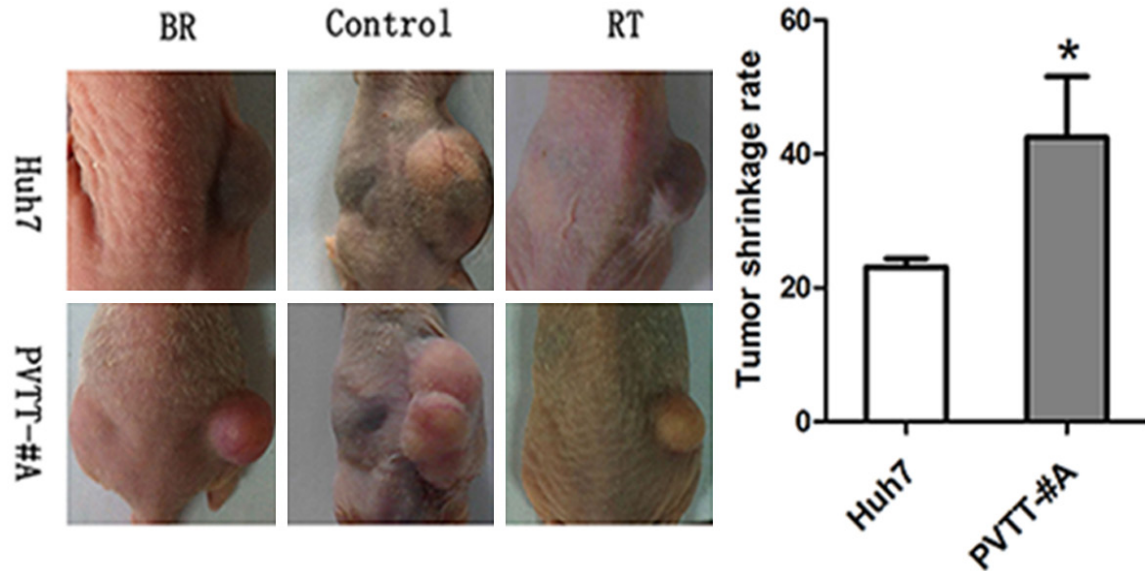


Figure 5. PVTTs are more sensitive to irradiation in nude mice. Left panel: representative images of mice before radiotherapy (BR), non-radiotherapy (control), and radiation (RT) after 3 weeks from left to right with 6 mice in each group; Right panel: histogram showing the shrinkage ratio of xenograft tumors derived from Huh7 and PVTT-#A cells compared with before radiotherapy. The shrinkage ratio of the xenograft tumors was calculated as $(\%) = [V(\text{BR}) - V(\text{RT})] / V(\text{BR})$. Data are presented as the mean \pm SD. * $P < 0.05$.

Huh7 and PVTT-#A cells and performed 3D-CRT on the subcutaneous tumors with fractionated irradiation at 18 Gy in 6 fractions. We compared tumor sizes before and after 3D-CRT for 3 weeks (**Figure 5**). The tumors derived from PVTT-#A cells shrunk after radiotherapy by $44.0\% \pm 4.17$, more than the $23.5\% \pm 3.42$ in tumors derived from Huh7 cells ($P < 0.05$). The results suggested that PVTT is more sensitive to radiation *in vivo*.

Irradiation inhibits the aggressive behavior of CSQT-2

In addition to promoting apoptosis and inhibiting the proliferation of cells, we explored the influence of irradiation on the migration of CSQT-2 cells in a wound healing experiment (**Figure 6A**) and a transwell migration assay (**Figure 6B**). We treated cells with a single dose of 6 Gy to decrease the experimental error, which induced fewer apoptotic and dead cells. From **Figure 6A**, the wound healing ability of CSQT-2 cells exposed to 6 Gy of irradiation did not significantly change compared with the control group at 24 h, but it decreased at 72 h ($P < 0.01$). Meanwhile, Hep3B and Huh7 cells

exposed to 6 Gy of irradiation showed enhanced wound healing ability compared with the control group at 24 h ($P < 0.01$), but it was not significantly different at 72 h. Transwell migration assay results showed that the number of CSQT-2 cells migrating through the chamber membrane was not significantly different between the control and irradiation at 24 h groups; however, the number of cells was lower in the irradiation for the 72 h group than the control group ($P < 0.01$). The number of Hep3B and Huh7 cells exposed to 6 Gy of irradiation at 24 h that migrated through the chamber membrane was more than that of the control group ($P < 0.01$) but less at 72 h ($P < 0.05$). Both findings showed that irradiation can inhibit the migration of CSQT-2 cells, but the migration capacity of HCC cells that were exposed to a single 6 Gy dose of irradiation revealed a time-dependent effect.

Discussion

Radiotherapy is one of the most commonly used therapeutic modalities in cancer treatment, but HCC has long been considered to be a radioresistant tumor [16]. Evidences accumu-

Radiosensitivity of PVTT

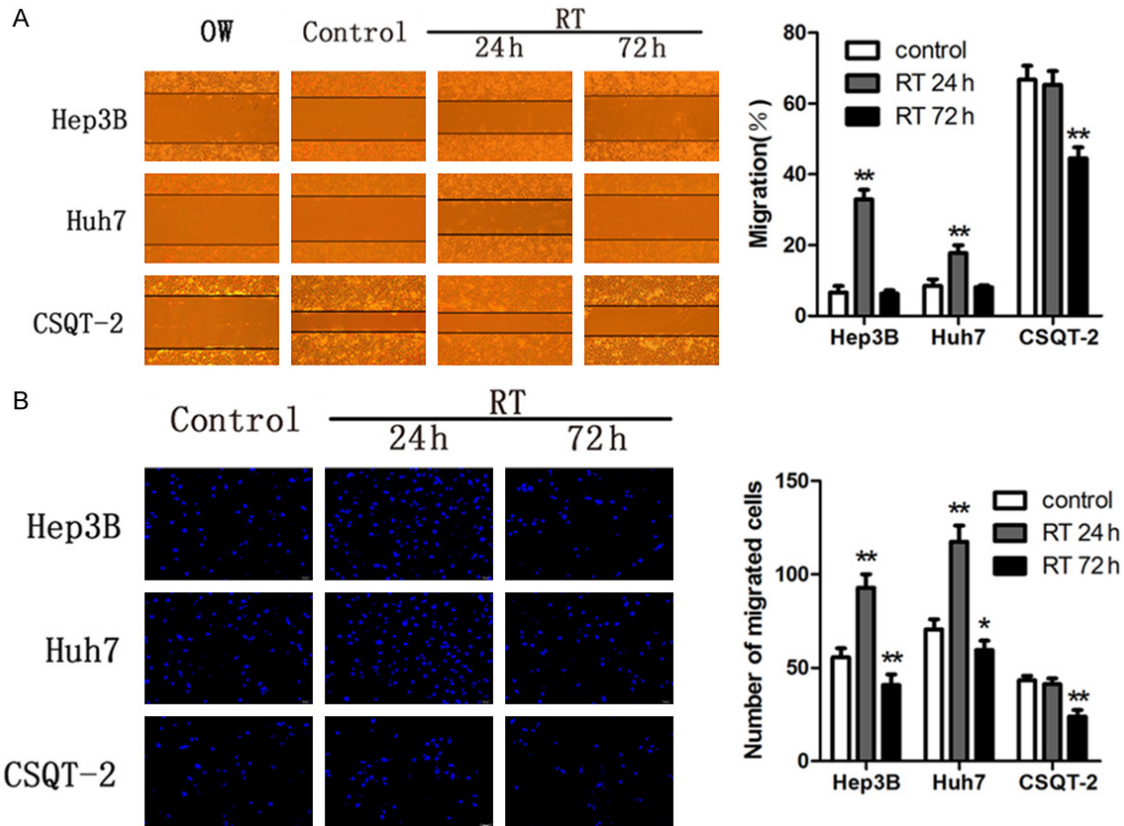


Figure 6. Irradiation inhibits the migration of CSQT-2 cells. A: Left panel: representative photomicrographs of the indicated treatments in cells by wound healing assay, images represent the original wound width (OW), the wound width of the non-radiation group (control), the wound width of the radiation group (RT) after 24 h or 72 h from left to right. Magnification 40 \times . Right panel: results of wound healing assay of each cell type for both the irradiation group and control group. Migration was calculated as (%)= $\frac{W(OW)-W(\text{control or RT})}{W(OW)}$. Data are presented as the mean \pm SD of 3 independent experiments. ** $P < 0.01$ versus the control. B: Left panel: Representative photomicrographs of the indicated cells, magnification 200 \times . Right panel: Quantification of average number of cells/field. Data are presented as mean \pm SD of 3 independent experiments. * $P < 0.05$, ** $P < 0.01$ versus the control.

lating in recent years have shown that radiotherapy for PVTT shows a relatively good curative effect [11-13]. Nevertheless, there is no experimental study focused on the radiosensitivity of PVTT and the modulation of biological behaviors by RT. In this study, we investigated the differential radiosensitivity among normal liver cells (HL-7702), HCC cells (Hep3B and Huh7) and PVTT cells (CSQT-2). Our results showed that PVTT is more radiosensitive than HCC both *in vitro* and *in vivo*. Moreover, we uncovered the critical effects of irradiation on PVTT cells, including a higher rate of apoptosis induced by irradiation and effects on suppressing the potential ability of proliferation and invasion in PVTT cells.

The lack of experimental cells originating from PVTT tissues may be responsible for the poor

understanding of the pathogenesis of PVTT induced by irradiation. Our group established a new cell line derived from PVTT (CSQT-2), which was used in this study. Our results show that the survival fraction was lower in CSQT-2 cells than HCC cells; this finding is consistent with the results of clinical studies [17, 18]. More importantly, our results uncovered that irradiation induced a higher rate of apoptosis and significantly more potential proliferative ability suppression in CSQT-2 cells than in Hep3B and Huh7 HCC cells. Although a previous study demonstrated that irradiation enhances the invasiveness of tumor cells [19], which this study also identified under low dose exposure of 6 Gy irradiation, our results showed that RT significantly inhibited the invasiveness of CSQT-2 cells. All of these results may explain why

HCC is a radioresistant tumor, but RT is a favorable treatment for PVTT.

Historical reports have shown that irradiation can activate caspase3 to split PARP (a type of DNA damage repair protein) into two fragments and participate in the apoptosis of HCC cells [20-22]. Irradiation can cause HCC cells to arrest in the G2/M phase [23], which is consistent with our results. However, our study is the first time that irradiation was shown to cause uniform effects on PVTT-originated cells. Furthermore, irradiation activates more caspase3 and splits more PARP in CSQT-2 cells, which explains why irradiation induces more apoptosis and death in CSQT-2 cells. In addition, we found that anti-apoptosis protein Bcl-2 levels were similar before and after irradiation, but the level of Bcl-2 was lower in CSQT-2 cells than Hep3B and Huh7 cells, indicating that the anti-apoptotic capacity of CSQT-2 cells is weaker than that of HCC cells. This finding further explains why CSQT-2 cells are more easily subjected to apoptosis. PCNA is an important molecule for cell proliferation [24, 25]; Piao LS *et al.* have reported that irradiation can down-regulate the level of PCNA in CD133⁺ HCC cells, but not in CD133⁻ HCC cells [26]. In our study, we found that the level of PCNA was down-regulated by irradiation in CSQT-2 cells, which contributed to inhibit their proliferation.

Irradiation-induced liver disease is one of the most common toxic effects of radiotherapy, and it is caused by irradiation affecting normal liver tissue around the tumor [27, 28]. In this study, we found that irradiation caused a higher rate of apoptosis and more strongly inhibited proliferation in normal HL-7702 liver cells than in Hep3B and Huh7 HCC cells, indicating that radiotherapy indeed induced an obvious toxic effect on normal cells. These results further suggested that RT used for primary HCC tumors or PVTT must be accurate in order to avoid damage to the surrounding liver tissue.

In conclusion, we first demonstrated that PVTT cells are more radiosensitive than HCC cells. RT induced a higher rate of apoptosis and strongly inhibited proliferation and invasion of PVTT cells. These results provides a further basis for clinical application of RT. Additionally, it is important to further explore the molecular mechanism of the differential response to RT between HCC and PVTT.

Acknowledgements

This work was supported by grants of the Science Fund for Creative Research Groups (No: 81221061); the State Key Project on Diseases of China (2012zx10002016016003); the China National Funds for Distinguished Young Scientists (No: 81125018, 81425019); the Chang Jiang Scholars Program (2013) of China Ministry of Education; the National Key Basic Research Program “973 project” (No: 2015CB554000); the China National Funds for National Natural Science Fund (No: 81101511, 81472282); the New Excellent Talents Program of Shanghai Municipal Health Bureau (No: XBR2011025); the Shanghai Science and Technology Committee (No: 134119a0200); the General Program from Shanghai Municipal Health Bureau (No: 20124301); the Shanghai Rising-star Program from Shanghai Science and Technology Committee (No: 13QA14049-00); the SMMU Innovation Alliance for Liver Cancer Diagnosis and Treatment (2012).

Disclosure of conflict of interest

None.

Address correspondence to: Drs. Shu-Qun Cheng and Yan Meng, Eastern Hepatobiliary Surgery Hospital, Second Military Medical University, 225 Changhai Road, Shanghai 200438, China. Tel: (86) 021-81875251; Fax: (86) 021-65562400; E-mail: chengshuqun@aliyun.com (SQC); Tel: 15902189-696; E-mail: yanmeng1121@163.com (YM)

References

- [1] Jemal A, Bray F, Center MM, Ferlay J, Ward E and Forman D. Global cancer statistics. *CA Cancer J Clin* 2011; 61: 69-90.
- [2] El-Serag HB and Rudolph KL. Hepatocellular carcinoma: epidemiology and molecular carcinogenesis. *Gastroenterology* 2007; 132: 2557-76.
- [3] Liu S, Guo W, Shi J, Li N, Yu X, Xue J, Fu X, Chu K, Lu C, Zhao J, Xie D, Wu M, Cheng S and Liu S. MicroRNA-135a contributes to the development of portal vein tumor thrombus by promoting metastasis in hepatocellular carcinoma. *J Hepatol* 2012; 56: 389-96.
- [4] Shi J, Lai EC, Li N, Guo WX, Xue J, Lau WY, Wu MC and Cheng SQ. A new classification for hepatocellular carcinoma with portal vein tumor thrombus. *J Hepatobiliary Pancreat Sci* 2011; 18: 74-80.

Radiosensitivity of PVTT

- [5] Tang QH, Li AJ, Yang GM, Lai EC, Zhou WP, Jiang ZH, Lau WY and Wu MC. Surgical resection versus conformal radiotherapy combined with TACE for resectable hepatocellular carcinoma with portal vein tumor thrombus: a comparative study. *World J Surg* 2013; 37: 1362-70.
- [6] Llovet JM and Bruix J. Novel advancements in the management of hepatocellular carcinoma in 2008. *J Hepatol* 2008; 48 Suppl 1: S20-37.
- [7] Chau GY, Lui WY and Wu CW. Spectrum and significance of microscopic vascular invasion in hepatocellular carcinoma. *Surg Oncol Clin N Am* 2003; 12: 25-34.
- [8] Lee DS and Seong J. Radiotherapeutic options for hepatocellular carcinoma with portal vein tumor thrombosis. *Liver Cancer* 2014; 3: 18-30.
- [9] Hou JZ, Zeng ZC, Zhang JY, Fan J, Zhou J and Zeng MS. Influence of tumor thrombus location on the outcome of external-beam radiation therapy in advanced hepatocellular carcinoma with macrovascular invasion. *Int J Radiat Oncol Biol Phys* 2012; 84: 362-8.
- [10] Kim JY, Chung SM, Choi BO and Kay CS. Hepatocellular carcinoma with portal vein tumor thrombosis: Improved treatment outcomes with external beam radiation therapy. *Hepatol Res* 2011; 41: 813-24.
- [11] Zeng ZC, Fan J, Tang ZY, Zhou J, Qin LX, Wang JH, Sun HC, Wang BL, Zhang JY, Jiang GL and Wang YQ. A comparison of treatment combinations with and without radiotherapy for hepatocellular carcinoma with portal vein and/or inferior vena cava tumor thrombus. *Int J Radiat Oncol Biol Phys* 2005; 61: 432-43.
- [12] Katamura Y, Aikata H, Takaki S, Azakami T, Kawaoka T, Waki K, Hiramatsu A, Kawakami Y, Takahashi S, Kenjo M, Toyota N, Ito K and Chayama K. Intra-arterial 5-fluorouracil/interferon combination therapy for advanced hepatocellular carcinoma with or without three-dimensional conformal radiotherapy for portal vein tumor thrombosis. *J Gastroenterol* 2009; 44: 492-502.
- [13] Zhang XB, Wang JH, Yan ZP, Qian S, Du SS and Zeng ZC. Hepatocellular carcinoma with main portal vein tumor thrombus: treatment with 3-dimensional conformal radiotherapy after portal vein stenting and transarterial chemoembolization. *Cancer* 2009; 115: 1245-52.
- [14] Wang T, Hu HS, Feng YX, Shi J, Li N, Guo WX, Xue J, Xie D, Liu SR, Wu MC and Cheng SQ. Characterisation of a novel cell line (CSQT-2) with high metastatic activity derived from portal vein tumour thrombus of hepatocellular carcinoma. *Br J Cancer* 2010; 102: 1618-26.
- [15] Feng YX, Wang T, Deng YZ, Yang P, Li JJ, Guan DX, Yao F, Zhu YQ, Qin Y, Wang H, Li N, Wu MC, Wang HY, Wang XF, Cheng SQ and Xie D. Sorafenib suppresses postsurgical recurrence and metastasis of hepatocellular carcinoma in an orthotopic mouse model. *Hepatology* 2011; 53: 483-92.
- [16] Curro G, Jiao L, Scisca C, Baccarani U, Mucciaridi M, Habib N and Navarra G. Radiofrequency-assisted liver resection in cirrhotic patients with hepatocellular carcinoma. *J Surg Oncol* 2008; 98: 407-10.
- [17] Kim DY, Park W, Lim DH, Lee JH, Yoo BC, Paik SW, Kho KC, Kim TH, Ahn YC and Huh SJ. Three-dimensional conformal radiotherapy for portal vein thrombosis of hepatocellular carcinoma. *Cancer* 2005; 103: 2419-26.
- [18] Yoon SM, Lim YS, Won HJ, Kim JH, Kim KM, Lee HC, Chung YH, Lee YS, Lee SG, Park JH and Suh DJ. Radiotherapy plus transarterial chemoembolization for hepatocellular carcinoma invading the portal vein: long-term patient outcomes. *Int J Radiat Oncol Biol Phys* 2012; 82: 2004-11.
- [19] Cheng JC, Chou CH, Kuo ML and Hsieh CY. Radiation-enhanced hepatocellular carcinoma cell invasion with MMP-9 expression through PI3K/Akt/NF-kappaB signal transduction pathway. *Oncogene* 2006; 25: 7009-18.
- [20] Tsang TY, Tang WY, Chan JY, Co NN, Au Yeung CL, Yau PL, Kong SK, Fung KP and Kwok TT. P-glycoprotein enhances radiation-induced apoptotic cell death through the regulation of miR-16 and Bcl-2 expressions in hepatocellular carcinoma cells. *Apoptosis* 2011; 16: 524-35.
- [21] Chen MF, Hsieh CC, Chen WC and Lai CH. Role of interleukin-6 in the radiation response of liver tumors. *Int J Radiat Oncol Biol Phys* 2012; 84: e621-30.
- [22] Yu W, Gu K, Yu Z, Yuan D, He M, Ma N, Lai S, Zhao J, Ren Z, Zhang X, Shao C and Jiang GL. Sorafenib potentiates irradiation effect in hepatocellular carcinoma in vitro and in vivo. *Cancer Lett* 2013; 329: 109-17.
- [23] Jin Y, Lyu Y, Tang X, Zhang Y, Chen J, Zheng D, Liang Y. Lupeol enhances radiosensitivity of human hepatocellular carcinoma cell line SMMC-7721 in vitro and in vivo. *Int J Radiat Biol* 2015; 91: 202-8.
- [24] Shen SQ, Li K, Zhu N and Nakao A. Expression and clinical significance of NET-1 and PCNA in hepatocellular carcinoma. *Med Oncol* 2008; 25: 341-5.
- [25] Gramantieri L, Trerè D, Chieco P, Lacchini M, Giovannini C, Piscaglia F, Cavallari A and Bolondi L. In human hepatocellular carcinoma in cirrhosis proliferating cell nuclear antigen (PCNA) is involved in cell proliferation and cooperates with P21 in DNA repair. *J Hepatol* 2003; 39: 997-1003.

Radiosensitivity of PVTT

- [26] Piao LS, Hur W, Kim TK, Hong SW, Kim SW, Choi JE, Sung PS, Song MJ, Lee BC, Hwang D and Yoon SK. CD133+ liver cancer stem cells modulate radioresistance in human hepatocellular carcinoma. *Cancer Lett* 2012; 315: 129-37.
- [27] Lawrence TS, Robertson JM, Anscher MS, Jirtle RL, Ensminger WD and Fajardo LF. Hepatic toxicity resulting from cancer treatment. *Int J Radiat Oncol Biol Phys* 1995; 31: 1237-48.
- [28] Cheng JC, Wu JK, Huang CM, Liu HS, Huang DY, Cheng SH, Tsai SY, Jian JJ, Lin YM, Cheng TI, Horng CF and Huang AT. Radiation-induced liver disease after three-dimensional conformal radiotherapy for patients with hepatocellular carcinoma: dosimetric analysis and implication. *Int J Radiat Oncol Biol Phys* 2002; 54: 156-62.